

Novel Method of Aluminum to Copper Bonding by Cold Spray

Si-Lin Fu¹ · Cheng-Xin Li¹ · Ying-Kang Wei¹ · Xiao-Tao Luo¹ · Guan-Jun Yang¹ · Chang-Jiu Li¹ · Jing-Long Li²

Submitted: 11 July 2017 / in revised form: 5 February 2018 / Published online: 26 March 2018
© ASM International 2018

Abstract Cold spray bonding (CSB) has been proposed as a new method for joining aluminum and copper. At high speeds, solid Al particles impacted the groove between the two substrates to form a bond between Al and Cu. Compared to traditional welding technologies, CSB does not form distinct intermetallic compounds. Large stainless steel particles were introduced into the spray powders as in situ shot peen particles to create a dense Al deposit and to improve the bond strength of joints. It was discovered that introducing shot peen particles significantly improved the flattening ratio of the deposited Al particles. Increasing the proportion of shot peen particles from 0 to 70 vol.% decreased the porosity of the deposits from 12.4 to 0.2%, while the shear strength of joints significantly increased. The tensile test results of the Al-Cu joints demonstrated that cracks were initiated at the interface between the Al and the deposit. The average tensile strength was 71.4 MPa and could reach 81% of the tensile strength of pure Al.

Keywords cold spraying · dissimilar metal joint · in situ shot peening · mechanical property · microstructure

Introduction

Joining dissimilar materials is necessary in a large number of fields (Ref 1-3). Because of high thermal and electrical conductivity and good corrosion resistance, Al and Cu are commonly used in the aerospace and electronics industries. Because of the cost and weight of Cu, partially replacing Cu with Al in certain devices is attractive (Ref 4, 5). A variety of welding processes have been utilized to join Cu and Al, and such processes have included diffusion welding (Ref 6), friction stir welding (Ref 7-10), laser welding (Ref 11), magnetic pulse welding (Ref 12), electron beam welding (Ref 3, 13), explosive welding (Ref 14-16), brazing (Ref 17), and resistance spot welding (Ref 18). However, brittle intermetallic compounds form during welding and lead to weld gaping and brittleness, which can negatively impact mechanical properties and can result in limitations of Al/Cu joints (Ref 19-23).

Cold spraying (CS) is a deposition process that produces coatings and bulk components. Metal particles are accelerated to a supersonic velocity by expanding a high-pressure gas (He, N₂, or air) through a converging-diverging nozzle to produce a deposit via solid-state impact of powders onto a substrate. This impact causes severe plastic deformation and heating (Ref 24, 25). Solid particles bond to the substrate via mechanical interlocking and metallurgical bonding (Ref 26-29). Cold spraying can be used to prepare coatings and repair damaged surfaces. Because of high deposition efficiency and compressive stress within deposits, cold spraying is also used for additive manufacturing. Specifically, the deposit can be built up successively without a thickness limitation when this method is used (Ref 30, 31), in contrast to methods based on electron beam or selective laser melting. Therefore, cold spraying can be used to bond some dissimilar materials, such as Cu and Al, and this is termed cold spray bonding (CSB). What makes

✉ Cheng-Xin Li
licx@mail.xjtu.edu.cn

¹ School of Materials Science and Engineering, Xi'an Jiaotong University, Xi'an 710049, Shaanxi, China

² School of Materials Science and Engineering, Northwestern Polytechnical University, Xi'an 710072, Shaanxi, China

CSB different from cold spraying is that deposits produced via CSB can be the main stressed part for bonding of dissimilar materials, and the thickness is not limited; in contrast, the coating on the surface of a substrate via conventional cold spraying cannot be the main stressed part, and the thickness is limited. Deposits are expected to be relatively dense and to have good uniformity and high bond strength.

During cold spraying, an in situ tamping effect occurs, in which high-speed particles impact onto deposited particles, and this densifies the coating. The same phenomenon was found with ceramic particles exerting a tamping effect to densify a metal-ceramic composite coating. Therefore, introducing a number of hard second-phase particles into spray powders improves deposit density and adhesion strength (Ref 32, 33). In our previous studies (Ref 34, 35), porosity was significantly reduced using in situ shot peen-assisted cold spraying. Increased particle velocity and increased temperature can also reduce porosity of the deposits and enhance interparticle bonding. Cold spray technology can produce high bond strength, which may enable the joining of dissimilar materials.

CSB has many advantages in joining dissimilar materials. In contrast to conventional welding technologies, deleterious and coarse intermetallic compounds at the bonding interface can be avoided when using CSB. Because spray powders are reactive and easily oxidizable, the advantages of high-speed and low-spraying temperature make CSB an effective process for preparing deposits with negligible oxidation and phase transitions (Ref 36). For deposition temperatures below the melting point, particles remain in the solid state throughout the entire process, and this can efficiently eliminate the melting-induced negative effects and unfavorable structural changes (Ref 32, 37–41). Moreover, the particle material can be selected to regulate the chemical composition of the deposit (joint).

In this study, it was proposed that CSB (spraying Al powders) can be used to achieve bonding of pure Al and Cu materials. Large-sized stainless steel particles (about 250 μm) were added to a soft Al powder (about 30 μm) to enhance the in situ tamping effect. High-speed impact of large-sized stainless steel particles improves poor inter-particle bonding of deposited pure Al particles, thereby enhancing the mechanical properties of the joint. The microstructure and performance of the CSB deposit were investigated.

Materials and Methods

Materials

Commercially pure aluminum (AA 1050) and pure copper plates (with a thickness of 8 mm) were used as substrates.

Figure 1 shows the irregular morphology and size distribution of the gas (N_2)-atomized 1050 Al powders (Youxiang Nonferrous Metals, Beijing, China); diameters of the pure Al powder particles ranged from 20 to 60 μm , with an average diameter of 41 μm . In addition, commercially available, spherical-shaped 1Cr13 stainless steel powders with an average size of 251 μm were used as shot peen particles (Fig. 2). The chemical compositions of the Al and Cu substrates and Al powder are shown in Table 1.

Cold Spray Deposition

Cold spray deposition was produced using a custom-made cold spray system. Substrates were first sandblasted with 30-mesh quartz sand at a compressed air pressure of 0.6 MPa and then degreased with alcohol before cold spraying. To determine the effects of shot peen particle content on the microstructure and mechanical properties of the deposits, 10, 30, 50, and 70 vol.% shot peen particles were introduced into the Al powder using mechanical mixing. Detailed spray parameters are listed in Table 2. A convergent-divergent Laval nozzle (made of WC-Co cermet) was used; the nozzle had a throat diameter of 2.0 mm, an outlet diameter of 6 mm, and a divergent section length of 150 mm. Figure 3 illustrates the preparation of the shear test specimens. Al powders were deposited on Al or Cu substrates, and the thickness of the sprayed deposits was more than 3 mm to satisfy the prerequisite for the dimensions of the shear test specimens. A sample of a certain size was then cut from the primary specimen to machine the final shear test specimen. Figure 4 shows a schematic diagram of CSB. Deposits (about 500 μm) were first sprayed perpendicular to the sloped surface and then deposited perpendicular to the horizontal surface of the substrate until the groove was filled with Al deposits.

Microstructural Characterization and Measurements of Mechanical Properties

Surface morphologies, cross-sectional microstructures, and fractures of the deposits were examined using scanning electron microscopy (SEM; MIRA3-LMH; TESCAN, Czech Republic). The linear density of shot peen particles was measured to evaluate the number embedded in the substrates. Figure 5 shows the calculation model used for the linear density of the particles. Their deposit porosity and linear density were estimated using image analysis and ImageJ software. Each sample was measured using 15 cross-section images. Vickers hardness testing was performed at the bonding interface of the polished cross-section with a load of 50-g force for a holding duration of 15 s. Figure 6(a) shows the dimensions of the shear test

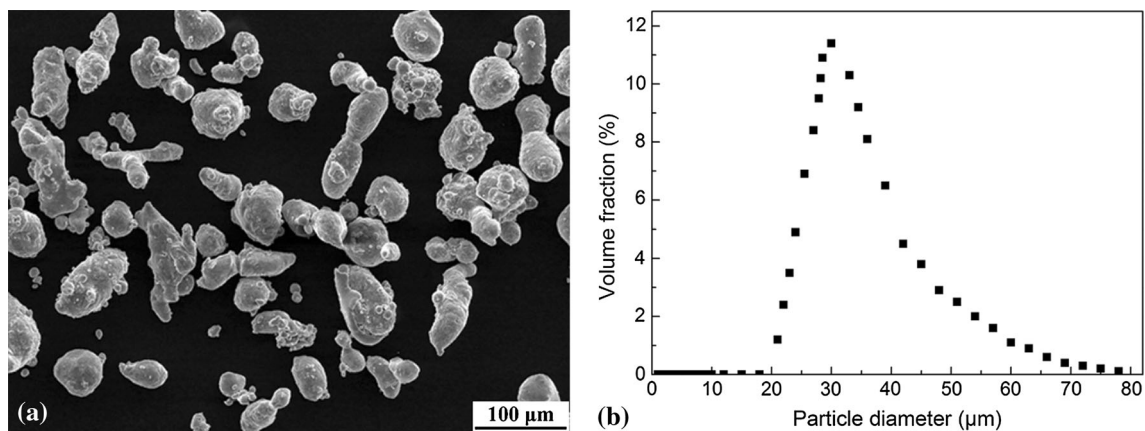


Fig. 1 Morphology (a) and size distributions (b) of Al powder

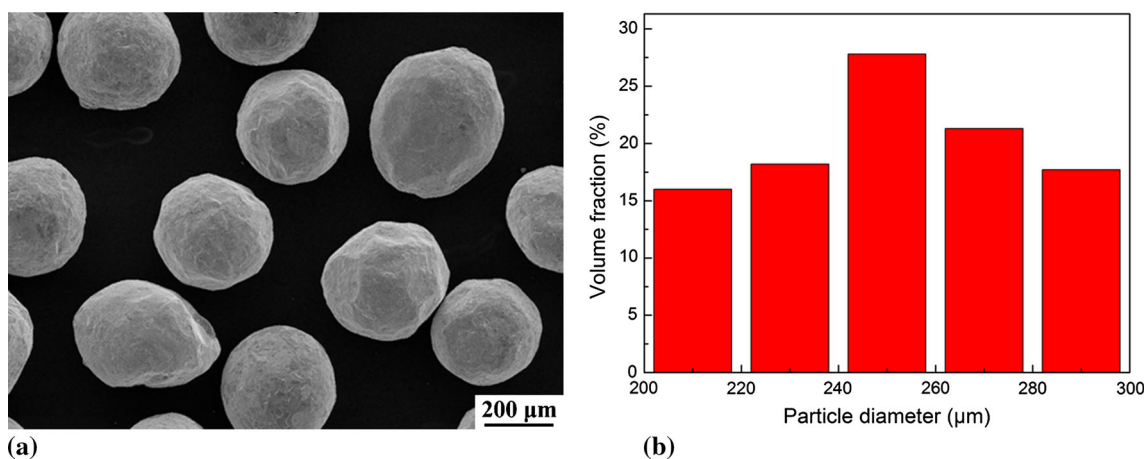


Fig. 2 Morphology (a) and size distributions (b) of stainless steel shot peen particles

Table 1 Chemical compositions of bulk Al, bulk Cu, and Al powder (wt.%)

Elements	Al	Cu	Zn	Ni	Fe	Si	Pb	Sn	O
Cu	0.11	Bal.	0.56	0.22	0.29	0.15	...
Al	Bal.	0.24	0.02	0.09	0.05	0.05
Al powder	Bal.	0.01	0.01	...	0.01	0.1	0.2

Table 2 Cold spraying parameters

Gas	Gas temperature, °C	Gas pressure, MPa	Gun traverse speed, mm/s	Standoff distance, mm	Powder feeder rate, g/min
N ₂	330	3	40	20	40

specimens, and Fig. 6(b) shows a schematic diagram of the shear test. Figure 7(a) provides the dimensions of the tensile test specimens, and Fig. 7(b) presents a schematic diagram of the tensile test. The shear strength and tensile tests were executed on a universal mechanical testing machine at loading speeds of 0.5 and 1 mm/min, respectively.

Results and Discussion

Effects of Shot Peen Particle Content on Microstructures of Al Deposits

Figure 8 shows cross-sectional microstructure and surface morphologies of the Al deposits. As presented in Fig. 8, the

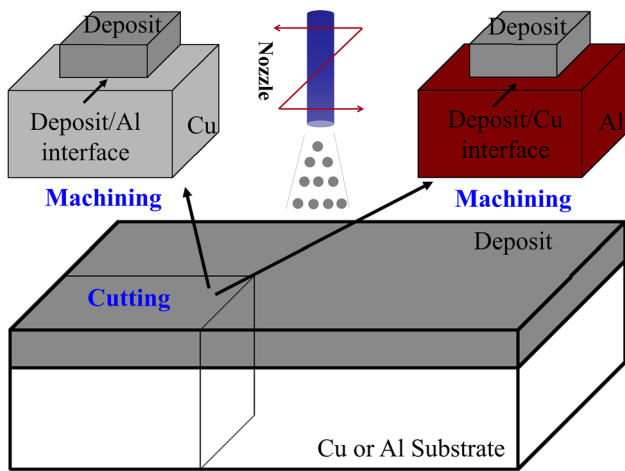


Fig. 3 Preparation of shear test specimens

Fig. 4 Schematic diagram of cold spray bonding

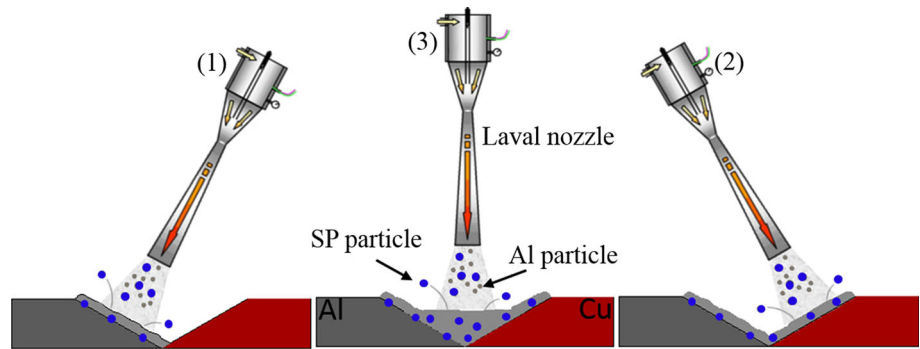
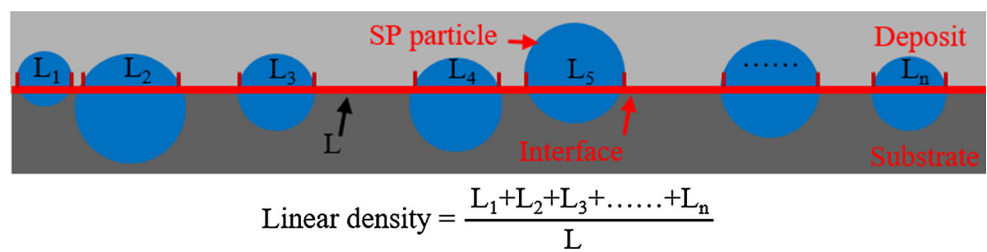


Fig. 5 Calculation model of the linear density of shot peen (SP) particles



shot peen particle content had a significant effect on the microstructure of the Al deposit. The pure Al coating (without shot peen particles) had a porous structure with numerous nearly spherical Al particles and open pores, and this suggests that the deformation of the Al particles was quite low during impact; consequently, poor bonding interfaces formed. With an increase in the shot peen particle content, the impacted regions (marked with red dashed lines) increased; severe plastic deformation of particles was sustained in these regions. Conversely, in the area without impact, the coating looks porous and shows a similar microstructure to the coating deposited without shot peen particles. When the shot peen particle content was 70 vol.%, the entire surface was sufficiently impacted, the deposit had a completely dense microstructure, and the

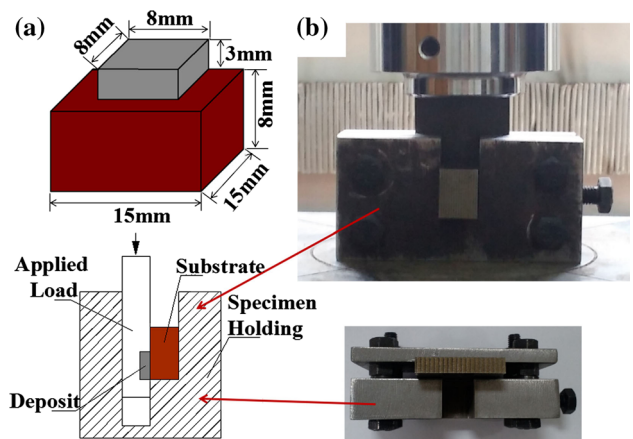


Fig. 6 Schematic diagrams and photographs of (a) shear test specimens and (b) the shear test

apparent pores disappeared. Flattening ratios of the Al particles in the deposits are shown in Fig. 9. The fraction of aluminum particles with a high flattening ratio increased as the shot peen particle content increased, and this was consistent with the microstructure. With the introduction of a certain content of hard particles into a soft feedstock, the porosity of the deposits decreased, and a similar densification effect was found (Ref 32–35).

Many efforts have been made to optimize the spraying parameters to reduce the porosity of Al deposits. Generally, a higher particle velocity and temperature are necessary to obtain dense Al coatings via cold spraying. Using helium as the accelerating gas (Ref 42) or improving gas pressure and temperature (Ref 43) are effective ways to achieve higher particle velocity. Additionally, it has been found

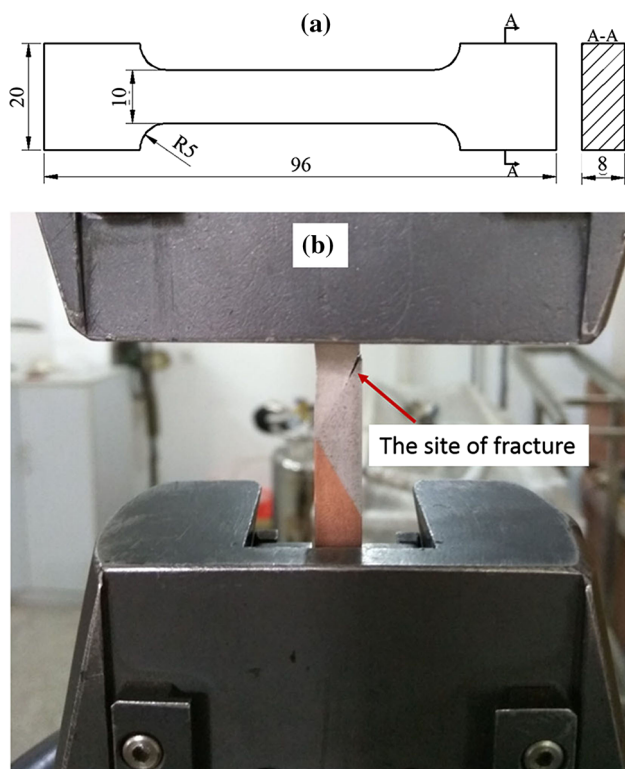


Fig. 7 Schematic diagram and photograph of (a) tensile test specimens and (b) the tensile test

that preparing a composite coating (Al-Al₂O₃) can effectively decrease porosity (~ 2%) (Ref 44). Figure 10 presents the porosity of Al deposits as a function of shot peen particle content. The average porosity was measured as 12.4% for the conventional process (without shot peen particles), whereas the porosities decreased as the shot peen particle content increased. The porosity decreased to 0.2% when the shot peen particle content was increased to 70 vol.%. This porosity value is lower than that (~ 0.5%) evaluated from a dense composite coating (Al-5%Mg) sprayed via helium (Ref 42). Therefore, the porosity decrease occurred because the pore size decreased when the impact-induced plastic deformation increased. The density of the Al deposit with shot peen particles can be compared to that of the deposit sprayed via helium.

Microhardness profiles across the interface between the deposit and the substrate are plotted in Fig. 11. With an increase in the shot peen particle content, the deposit microhardness gradually increased. Nevertheless, the microhardness of the deposits obtained using powders with the same shot peen particle content was almost the same on both Al and Cu substrates. Also, the hardness of the substrate decreased as the distance from the bonding interface increased until reaching the bulk value (approximately 200 μm below the interface). This was because of grit-

blasting and the tamping effect of Al and shot peen particle impact, which is similar to the shot peen process (Ref 35).

Differences in microhardness between the pure Al deposit and the bulk counterparts are because of work hardening and deposit porosity. During spraying, deposited Al particles can be impacted by the shot peen particles. Specifically, a greater content of shot peen particles results in denser deposits, more severe plastic deformation, and stronger grain refinement; therefore, the hardness is greater. In our previous studies (Ref 34), we investigated the impact of a shot peen particle on hardening and densification of the coating material up to a depth of about 300 μm . Therefore, continuous impact of shot peen particles during the deposition process ensures that all the deposited pure Al particles are hardened and experience equivalent work hardening. Consequently, it is clear that introducing shot peen particles can substantially increase the microhardness of both the deposit and substrate.

Effects of Shot Peen Content on Shear Strength of the Bonding Interface

The shear strength of the interface between the deposit and the substrate was measured (Fig. 6). Figure 12 shows a schematic diagram of the bonding interface. When the shot peen particle content was increased from 0 to 70 vol.%, the shear strength of the deposit/Al interface increased from 8.4 to 68.0 MPa and that of the deposit/Cu interface increased from 8.8 to 90.3 MPa. As seen in Fig. 13, when the deposit was sprayed with mixed powders containing 10 and 30 vol.% of shot peen particles, the shear strength of the deposit/Al interface was slightly higher than that of the deposit/Cu interface. In contrast, when the shot peen particle content was increased to 50 and 70 vol.%, the shear strength of the deposit/Al interface was lower than that of the deposit/Cu interface.

Figure 14 shows shear fracture morphologies of the interfaces between the substrates and deposits for specimens sprayed with powder mixtures containing 30 vol.% shot peen particles. The values of the shear strength of the deposit/Cu and deposit/Al interfaces are about 36.7 and 41.1 MPa, respectively. The substrate/deposit interface consisted of two parts: (1) the substrate/shot peen particle interface and (2) the substrate/Al particle interface. As shown in Fig. 14(a) and (b), the pit caused by shot peen particle impact on the Al substrate was deeper than that on the Cu substrate. The shot peen particles slid gradually in the direction of the force, and there were some deeper scratches on the Al substrate. In contrast, the shot peen particles slid on the Cu substrate, simply leaving some shallow pits without apparent scratches. The deeper scratches and larger number of these scratches on the surface of the substrate mean a higher shear force is needed.

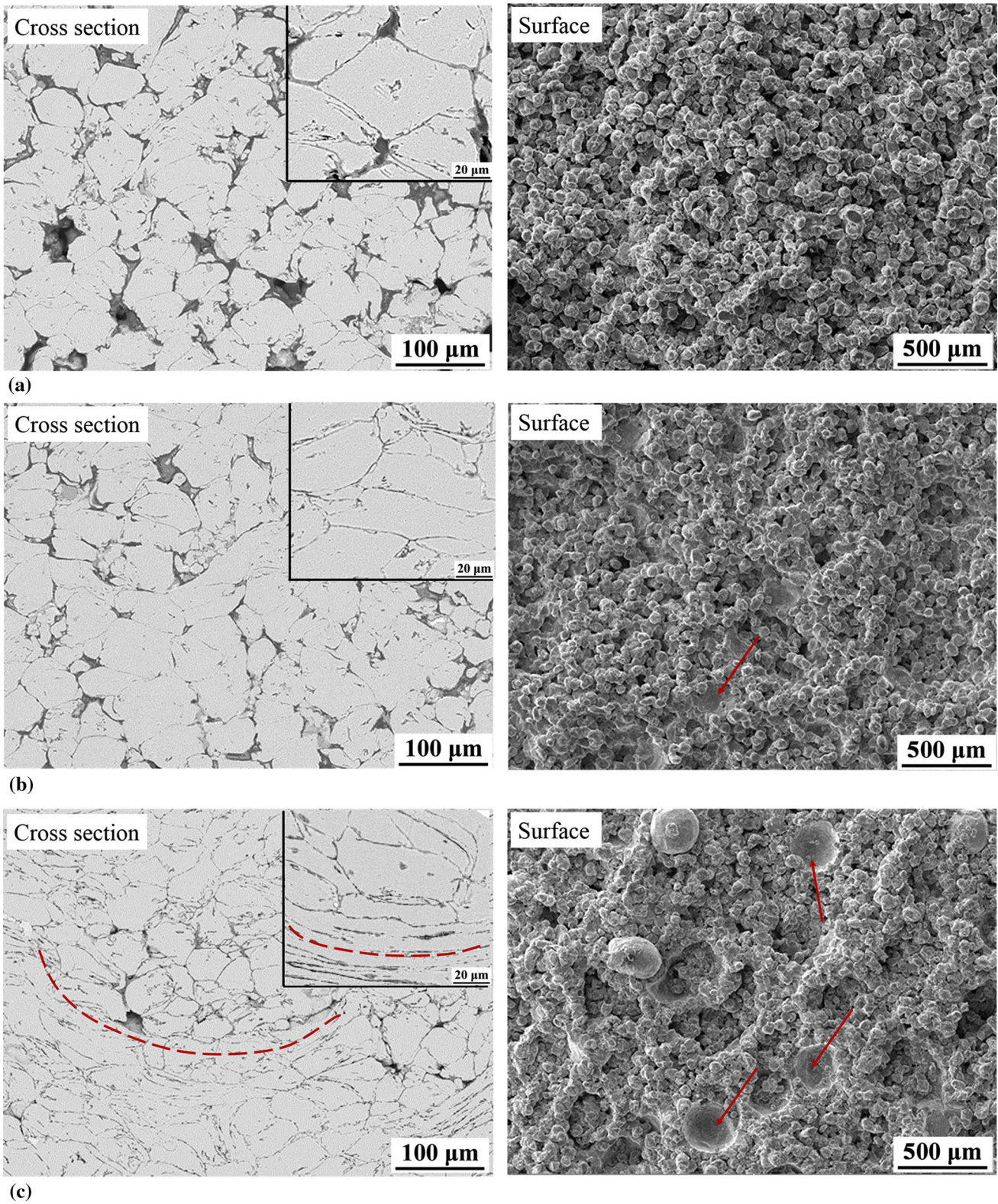


Fig. 8 Cross-sectional microstructures and surface morphologies of Al deposits sprayed using cold spraying assisted by in situ shot-peening: (a), (b), (c), (d) and (e) correspond to deposits prepared using powders with shot peen particle contents of 0, 10, 30, 50 and 70 vol.%, respectively

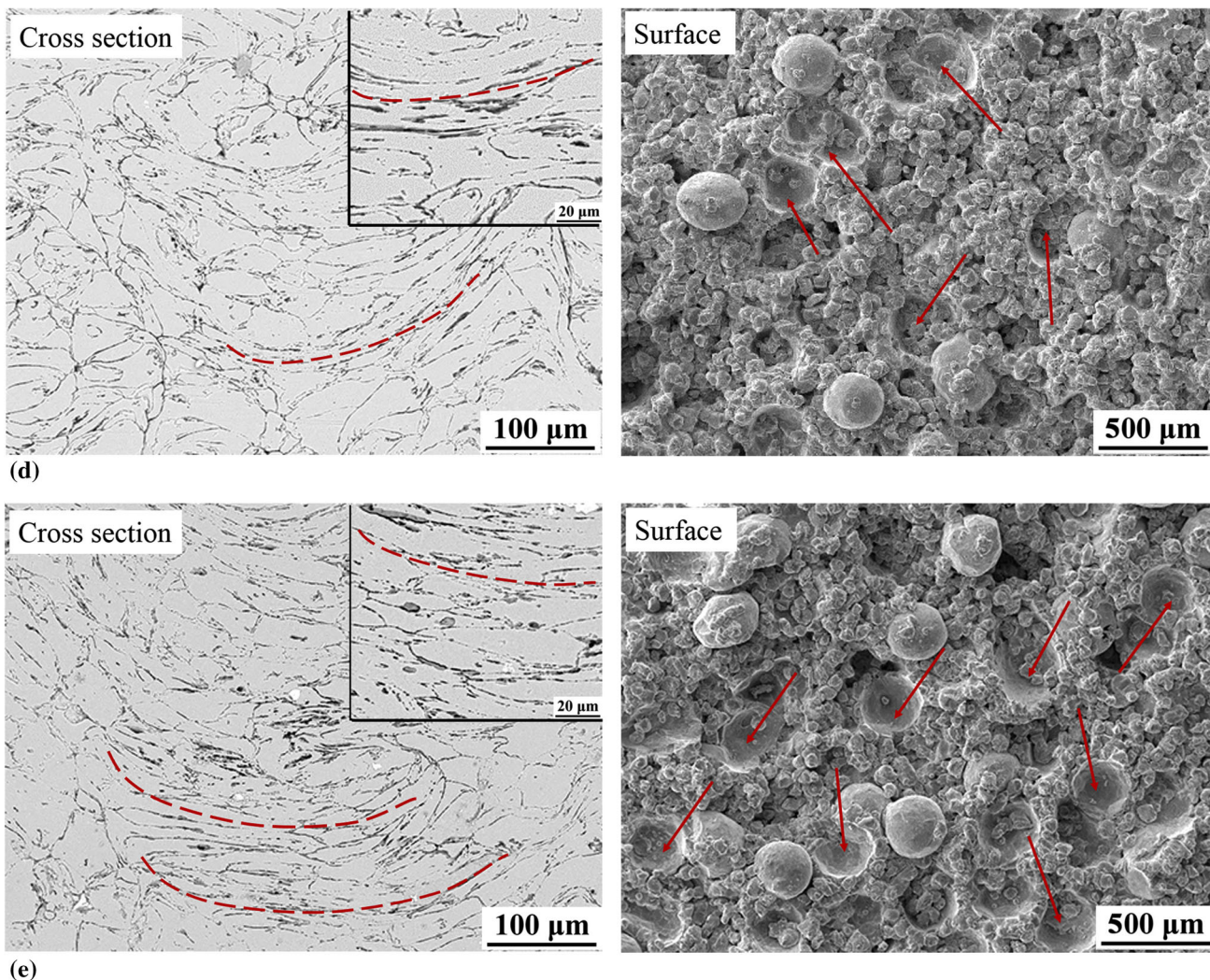


Fig. 8 continued

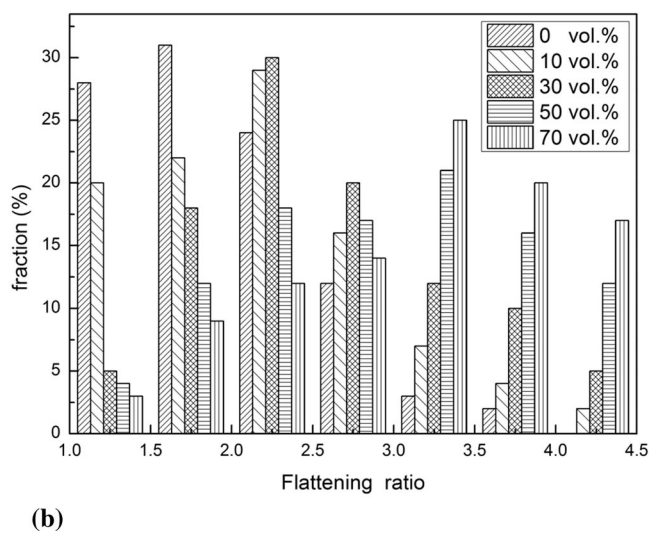
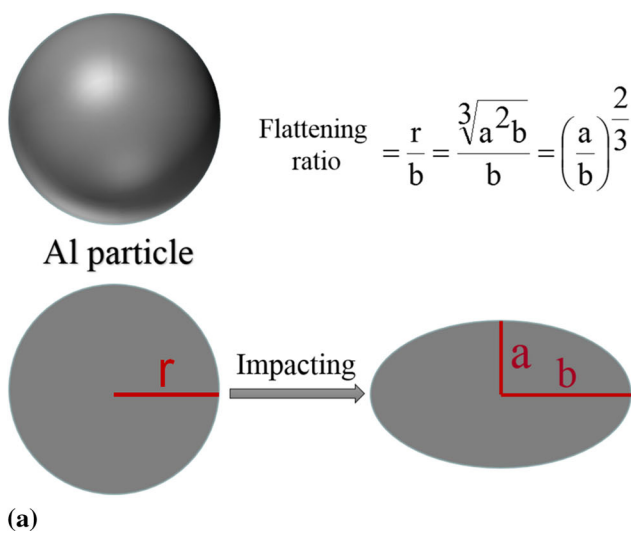


Fig. 9 Flattening ratios of pure Al particles in the deposits. (a) Calculation model of flattening ratio and (b) distribution of flattening ratios in deposits sprayed using pure Al powder and powder mixtures with different proportions of shot peen particles

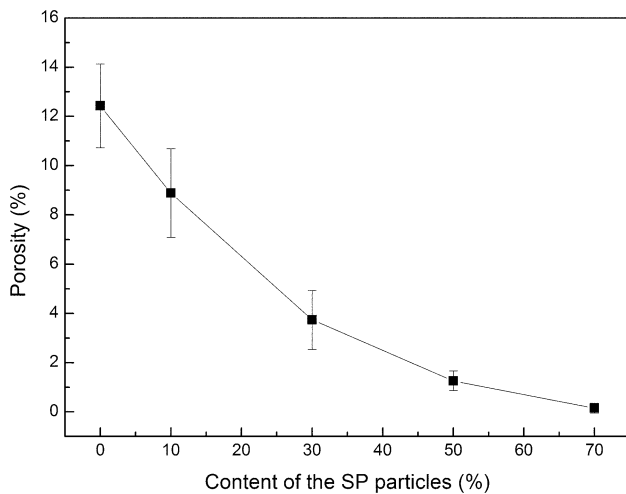


Fig. 10 Effects of shot peen particle content on the porosity of Al deposits

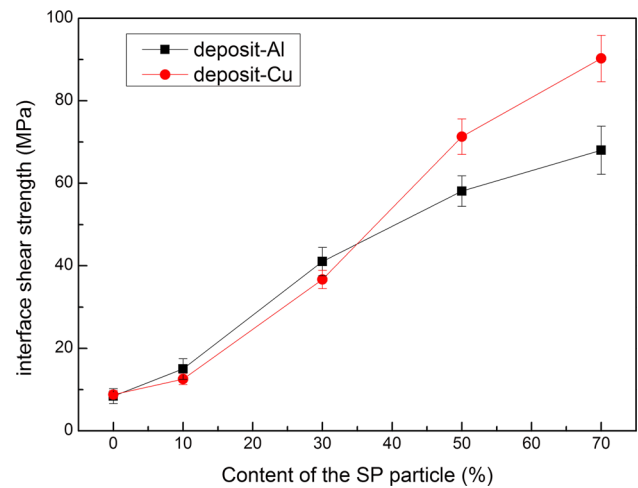


Fig. 13 Effects of shot peen particle content on the shear strength of deposit/substrate interfaces

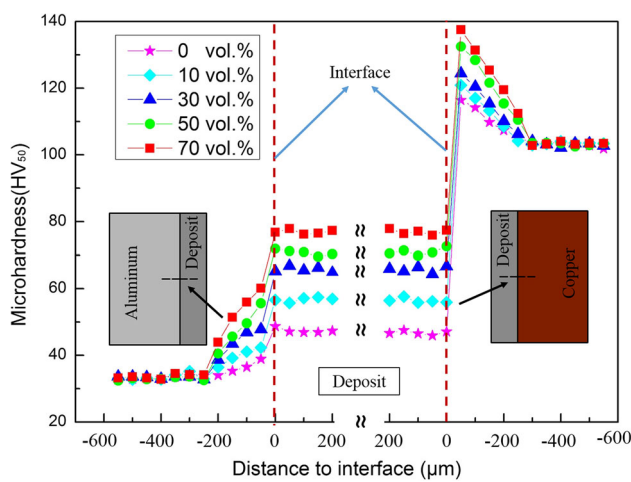


Fig. 11 Vickers microhardness along the deposit/substrate cross-sections

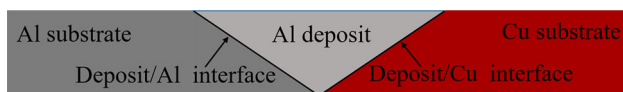


Fig. 12 Schematic of the bonding interface

Figure 15 shows cross-sectional microstructure of the interfaces between the substrates and the deposits sprayed with powder mixtures with 30 vol.% shot peen particles. From Fig. 15, it can be observed that some shot peen particles were embedded in the Al substrate. In contrast, because of the higher hardness of Cu compared to Al, almost all of the shot peen particles bounced off the Cu substrate surface. The density of the shot peen particles embedded at the deposit/substrate interface is presented in Fig. 16 as a function of the amount of shot peen particles in the original feedstock powder. The linear density of the

shot peen particles along the deposit/Cu interface was close to zero with only slight changes when the shot peen particle content was increased, whereas the shot peen particle density of the deposit/Al interface increased rapidly when the shot peen particle content was increased. These results demonstrate that the interlocking effect from the shot peen particles embedded in the Al substrate can effectively enhance the shear strength of the deposit/Al interface; in contrast, the effect on the deposit/Cu interface was slight. Also, for the deposit produced with mixed powders containing 10–30 vol.% shot peen particles, the pure Al particles exhibited low plastic deformation (Fig. 8b and c). Moreover, the bond strength of the interface between the deposited Al particles and the substrate was lower. Subsequently, the interlocking effect played a major role with respect to the shear strength, and, consequently, the shear strength of the deposit/Al interface was higher than that of the deposit/Cu interface. A model of the shot peen particle effect on the shearing process is shown in Fig. 17.

Figure 18 presents shear fracture morphologies of the deposit/Cu interface on the deposit side; the morphologies were observed via secondary electrons (SE). Low plastic deformation of the deposited Al particles and poor interfaces between those particles were observed in the deposits produced via spraying with mixed powders that contained 10 vol.% shot peen particles, and the shear strength was about 12.5 MPa. The shear fracture surface did not have apparent scratches under the action of shearing load. With an increase in the shot peen particle content to 50 vol.%, apparent interfaces between the particles were absent, and the shear fracture formed apparent scratches; the shear strength was about 71.3 MPa, which was a great improvement. Deposited Al particles experienced severe plastic deformation because of the hammering effect caused by in situ shot peening, and this resulted in a high

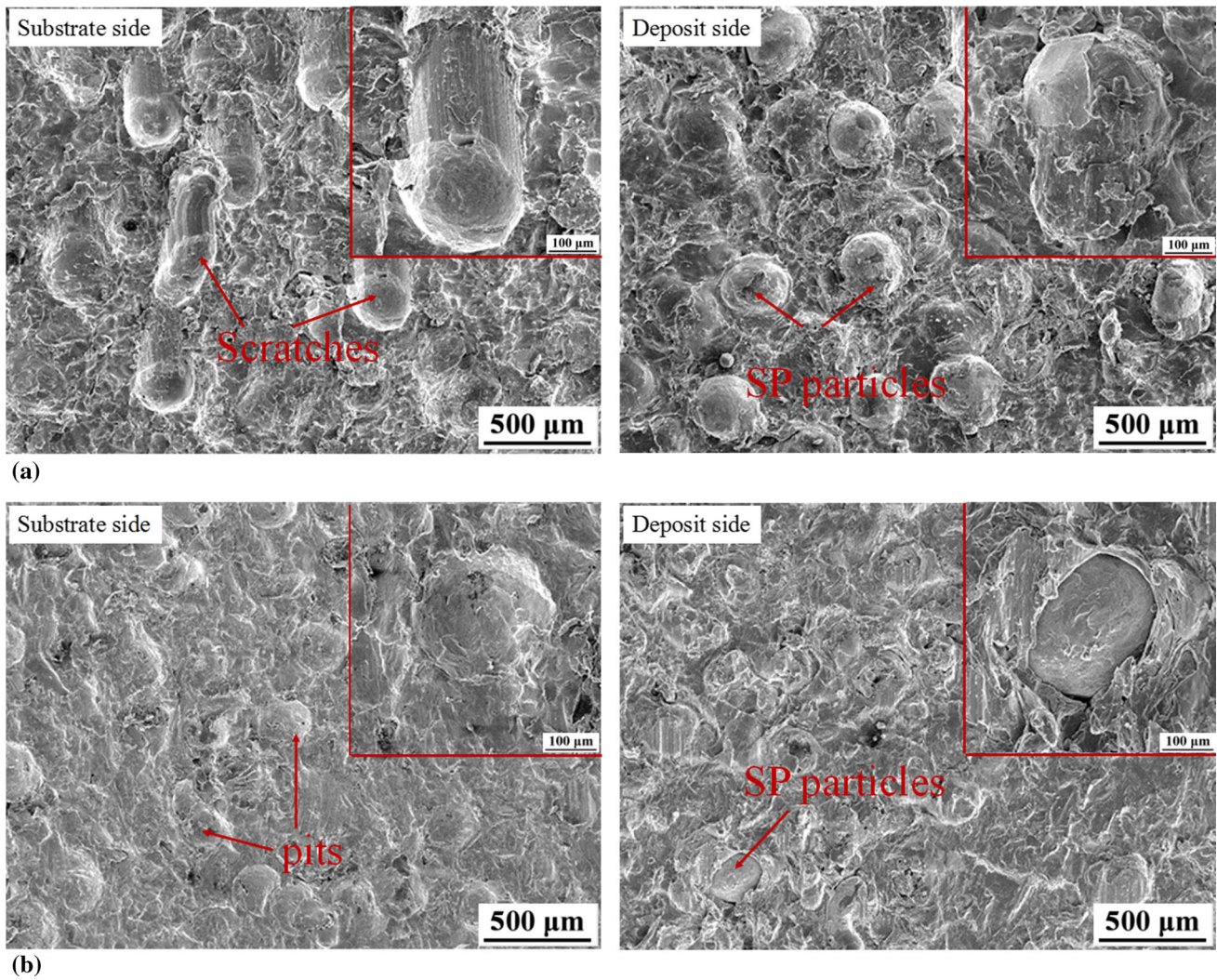


Fig. 14 Morphologies of shear fractures of the interfaces between the substrates and the deposits sprayed with powder mixtures containing 30 vol.% shot peen particles: (a) deposit/Al interface and (b) deposit/Cu interface

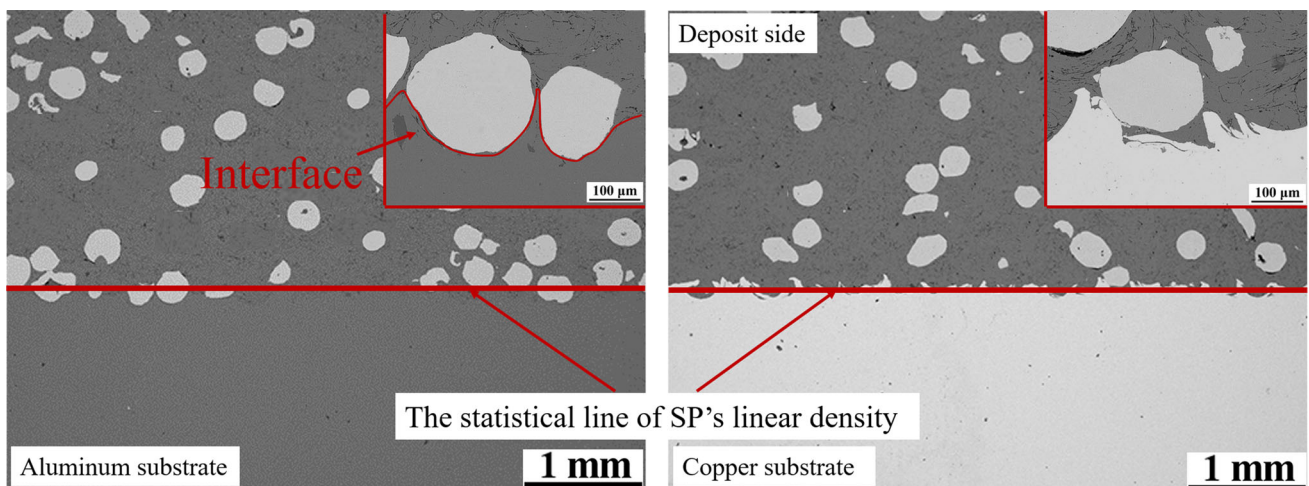


Fig. 15 Cross-sectional microstructure of the interfaces between the substrates and the deposits sprayed with powder mixtures containing 30 vol.% shot peen particles

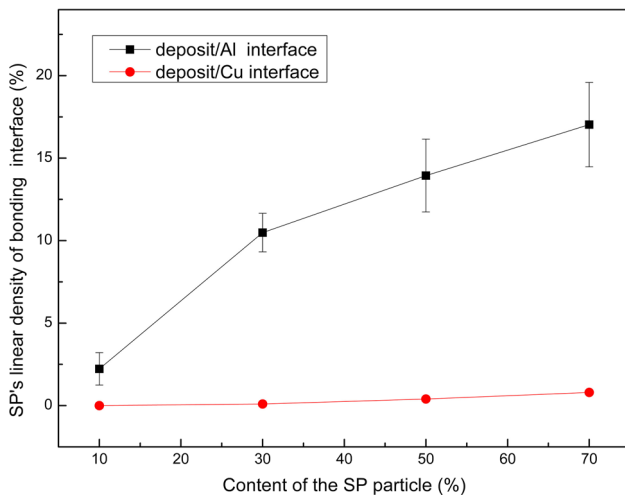


Fig. 16 Linear density of shot peen particles along the interfaces between the substrates and the layers deposited with pure Al powder and powder mixtures containing different proportions of shot peen particles

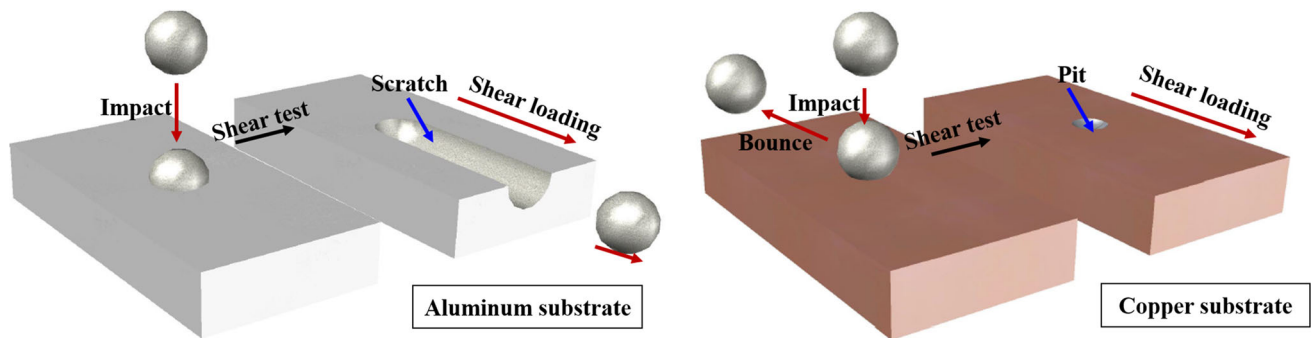


Fig. 17 Model of the effects of shot peen particles on the shearing process

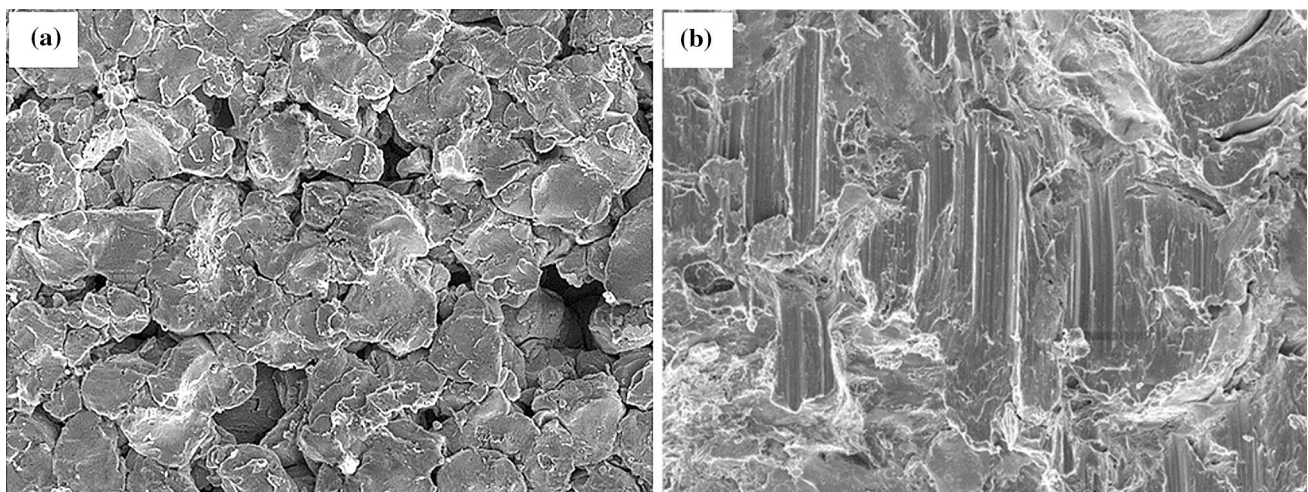


Fig. 18 Morphologies of the shear fractures of the deposit/Cu interface on the deposit side. The morphologies were observed via SE. (a) 10 vol.% shot peen particles and (b) 50 vol.% shot peen particles

bond strength between the deposited Al particles and the substrate. Under the action of shearing load, the deposit and substrate scratched against each other, thus forming apparent scratches. This suggests that the bond strength was stronger, which greatly increased the shear strength of the deposit/substrate interface.

As shown in Fig. 19, residual particles on the Cu substrate side of the shear fracture increased with an increase in the shot peen particle content. Figure 20 presents the shear fracture morphologies of the interface between the Cu substrates and the deposits sprayed with powder mixtures containing 50 vol.% shot peen particles; the morphologies were observed using back-scattered electrons (BSE); white regions shown in Fig. 19 represent Cu, and gray regions represent Al. A high amount of deposited Al particles were present on the Cu substrate side (Fig. 20a), and some fractured Cu fragments were present on the deposit side (Fig. 20b) of the shear fracture. These results

Fig. 19 Macro-shear fracture appearance of deposit/Cu interfaces

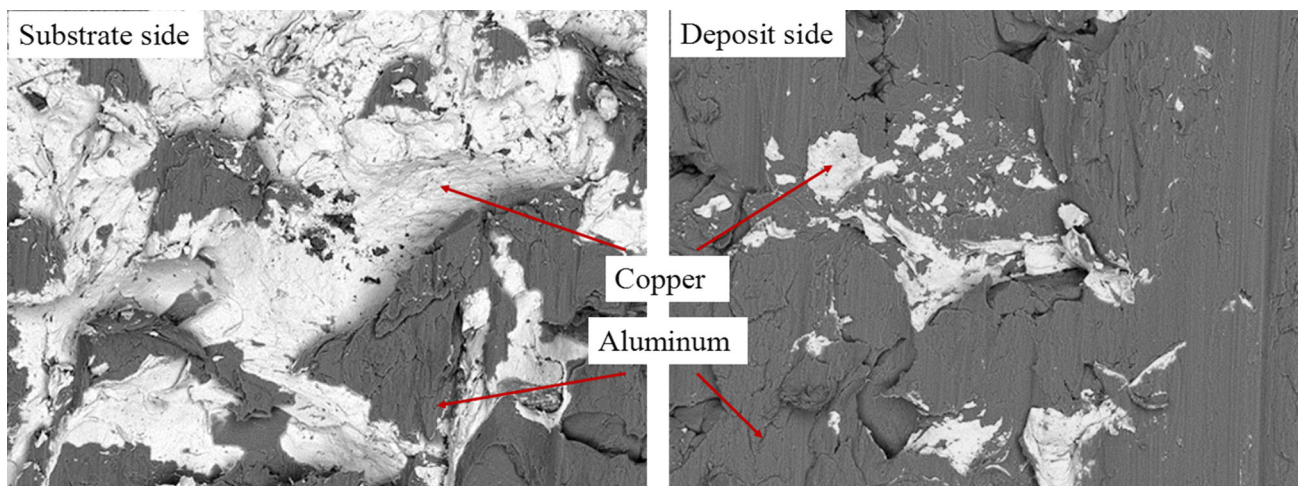
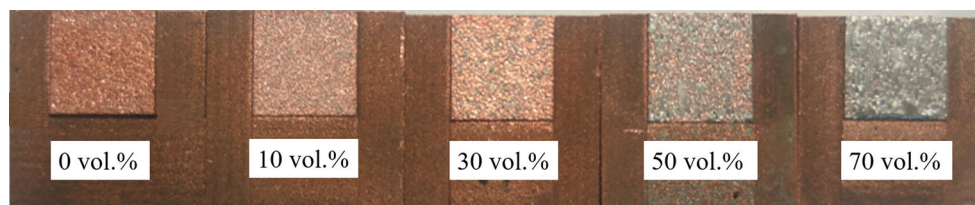


Fig. 20 Morphologies of shear fractures of the interface between the Cu substrate and the deposits sprayed with a powder mixture containing 50 vol.% shot peen particles. The morphologies were observed using BSE

demonstrate that not all of the fracture occurred along the deposit/Cu interface. Furthermore, fractures occurred inside the Cu substrate and inside the Al particle, and this suggests a high bond strength at the deposit/Cu interface. Therefore, the shear strength of the deposit/Cu interface was mainly caused by bonding between the deposited Al particle and the Cu substrate. For the Al substrate, the shear strength first increased rapidly with the addition of shot peen particles and then increased more slowly as the shot peen particle content was increased. When the deposit was produced with mixed powders containing 50–70 vol.% shot peen particles, the number of particles embedded in the Al substrate increased. Meanwhile, the pure Al particles exhibited severe plastic deformation (Fig. 8d, e), and the bond strength of the interface between the deposited Al particles and the substrate was higher. Hence, the shear strength of the deposit/Al interface was mainly caused by bonding between the deposited Al particles and the Al substrate, and by the interlocking effect of the shot peen particles embedded in the Al substrate. Also, the hardness near the interface of the Cu substrate was twice the hardness of the Al substrate (Fig. 11), and the deformation and fracture of the Cu substrate required higher forces than those of the Al substrate under the shearing process. Therefore, when the shot peen particle content was increased to 50–70 vol.%, the shear strength of the deposit/Al interface was lower than that of the deposit/Cu

interface. Table 3 summarizes the effects of shot peen particle content on the shear strength of the bonding interfaces.

Effects of Spray Angle on Shear Strength of the Bonding Interface

The spray angle was defined as the angle between the nozzle axis and the substrate surface. A schematic diagram of the spray angle is shown in Fig. 21. Figure 22 shows the effects of the spray angle on the deposition efficiency of pure Al deposits sprayed with powder mixtures containing 70 vol.% shot peen particles. As expected, there is an upward trend with an increase in spray angle. Powders that impact the substrate surface perpendicularly yield the highest deposition efficiencies of 32.3% (Cu) and 31.2% (Al). We also found that the two substrates, on average, have little or no effect on deposition efficiency. Figure 23 presents the effects of spray angle on the interface shear strength of pure Al deposits sprayed onto both Al and Cu substrates with powder mixtures containing 70 vol.% shot peen particles. The deposit/substrate interface shear strength gradually increased as the spray angle increased. When the spray angle decreased to 45°, the shear strength of the deposit/Cu and deposit/Al interfaces decreased to 78 MPa and 55 MPa, respectively.

Table 3 Summary of the effects of shot peen particle content on the shear strength of bonding interfaces

Shot peen content	Shear strength of interface	Major effect factor
10 vol.%, 30 vol.%	Deposit/Al > deposit/Cu	The interlocking effect by the shot peen particles
50 vol.%, 70 vol.%	Deposit/Al < deposit/Cu	The bond strength between the Al particles and the substrate, and the interlocking effect by the shot peen particles

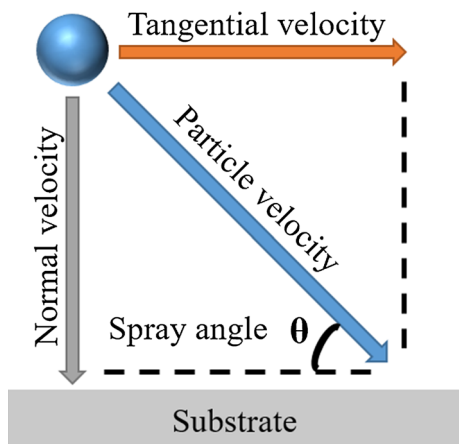


Fig. 21 Schematic of the spray angle

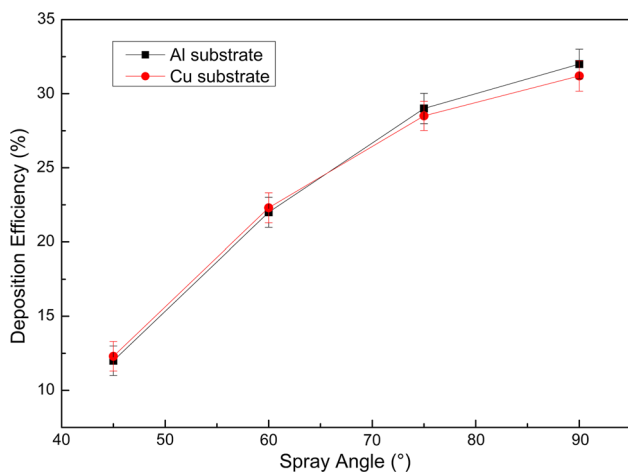


Fig. 22 Effects of spray angle on deposition efficiency of Al deposits sprayed with powder mixtures containing 70 vol.% shot peen particles

In cold spraying, particle velocity is a combination of tangential velocity and normal velocity. The tangential velocity component has a negligible effect on particle deposition, and, thus, particle deposition mainly depends on the normal component (Ref 45, 46). As the spray angle decreased from the normal angle, the tangential component of the particle velocity increased and the normal component decreased. When particles have normal velocities lower than the critical velocity, the particles do not deposit, and, inevitably, the particles blast and remove the

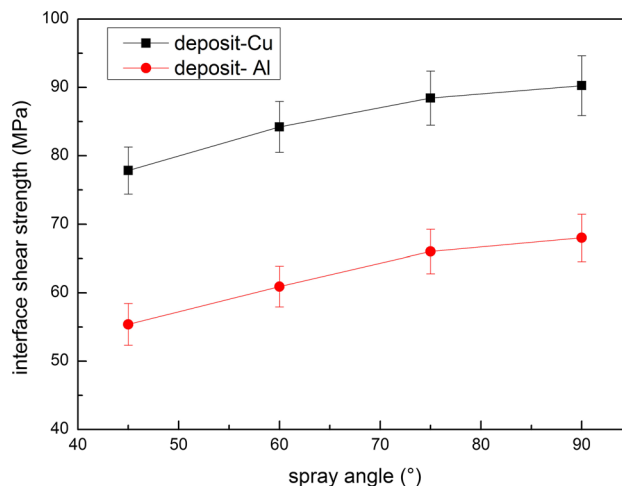


Fig. 23 Effects of spray angle on the interface shear strength between the substrates and the Al deposits sprayed with the powder mixture containing 70 vol.% shot peen particles

deposited layer. The deposited layer is also removed by the tangential movement of particles. Therefore, under the same spraying conditions, particles that have a larger normal velocity and smaller tangential velocity always result in higher deposition efficiency and shear strength.

Tensile Testing of Joining Pure Al to Cu by Cold Spray Bonding

On the basis of the above experimental results, the Al/Cu joint was designed as shown in Fig. 4. A series of tensile tests were conducted on complete joints sprayed with powder mixtures containing 70 vol.% shot peen particles. As observed in Fig. 7(b), the initial fracture location of the tensile test was the interface between the deposit and Al substrate. Figure 24 presents the morphologies of the specimens before and after the tensile test. The average tensile strength of the joint was 71.4 ± 1.5 MPa and was as high as 81% of the Al tensile strength.

Figure 25 shows the ratio of the joint tensile strength to base Al. Many efforts have been made to join Al to Cu using welding. However, it has always been difficult to join the two because of the enormous differences between Al and Cu. Otten et al. investigated an Al-Cu joint using electron beam welding and showed that the joint had good

Fig. 24 Morphologies of specimens before and after the tensile test

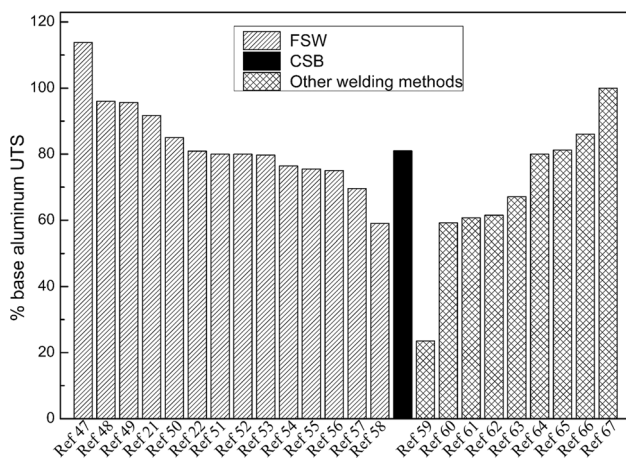
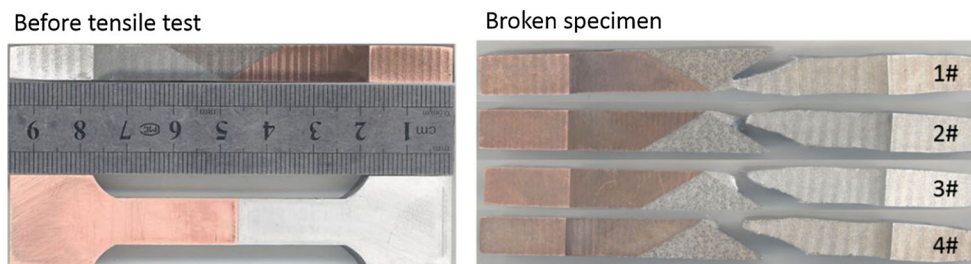


Fig. 25 Comparison between the ratio of the tensile strength of the CSB joint to the ultimate tensile strength of the base Al and the values of the ratios reported for Al/Cu joints prepared using other welding methods

mechanical strength: the ratio of the joint strength to Al strength is about 85%, which is greater than that obtained via many fusion welding processes (Ref 47). Solid-state welding processes (such as friction stir welding, ultrasonic welding, and diffusion welding) are effective methods that are usually used to join dissimilar materials such as Al and Cu. Much research has been reported on the use of friction stir welding technology to join Al-Cu material couples, and the ratio of the joint strength to Al strength changes remarkably (about 60–114%) when different parameters are used (Fig. 25) (Ref 21, 22, 48–59). Recent studies (Ref 61–63) have revealed that a ratio around 60% was obtained for the joints using an ultrasonic-assisted method. The dissimilar Al-Cu materials have been joined using laser braze welding (Ref 65, 66), and the ratio has been as high as approximately 80%. Therefore, using CSB to join dissimilar Al-Cu materials has certain advantages in terms of the strength ratio of the joint.

Figure 26 presents the tensile fracture morphologies at the deposit/substrate interface. The fracture of the interface between the Al substrate and the deposit consisted of two parts: (1) some of the fracture occurred at the interface between the deposited Al particles and the Al substrate, and (2) some of the fracture occurred between the shot

peen particles and the Al substrate because of the weak bond strength. There were a large number of pits with scratches on the Al substrate side of the fracture, such as in the shear fracture (Fig. 26b). For clarification, the force analysis of the tensile test is given in Fig. 27. The applied force was a combination of the tangential force and the normal force. On the Al substrate that had scratches, the particles moved in the direction of the tangential force. Therefore, the tensile strength consisted of the shear strength in the tangential direction and the bond strength in the normal direction. From Fig. 26 and 28, it can be observed that the dimple fracture morphology (indicated by red line ellipses) was concentrated near the impact zone of the shot peen particles, where the Al particles sustained strong plastic deformation because of shot peen particle impact and therefore achieved high bond strength. Not all of the fracture between the Al substrate and the deposited Al particles was ductile, and there was dimple fracture only in certain areas where strong plastic deformation of the particles occurred. As a consequence, the tamping effect of shot peening can result in severe plastic deformation of the deposited Al particles and can densify the deposit, conferring it with high bond strength; this is beneficial for the tensile strength when joining dissimilar Al-Cu materials. Meanwhile, the deposit unavoidably contains embedded shot peen particles. The interface between the shot peen particles and the Al substrate fractures easily because of its weak bonding strength (Fig. 26), but it is not the main factor that affects the tensile strength.

Conclusions

An exhaustive study of pure Al deposits on copper and aluminum substrates was carried out using in situ shot peen-assisted cold spraying, and the following conclusions were drawn from the present investigation:

1. Introducing shot peen particles into the powder is an effective approach for enhancing the density of pure Al deposits. As the proportion of shot peen particles was increased from 0 to 70 vol.%, the fraction of Al particles with a high flattening ratio gradually increased, the porosities of the deposit decreased from

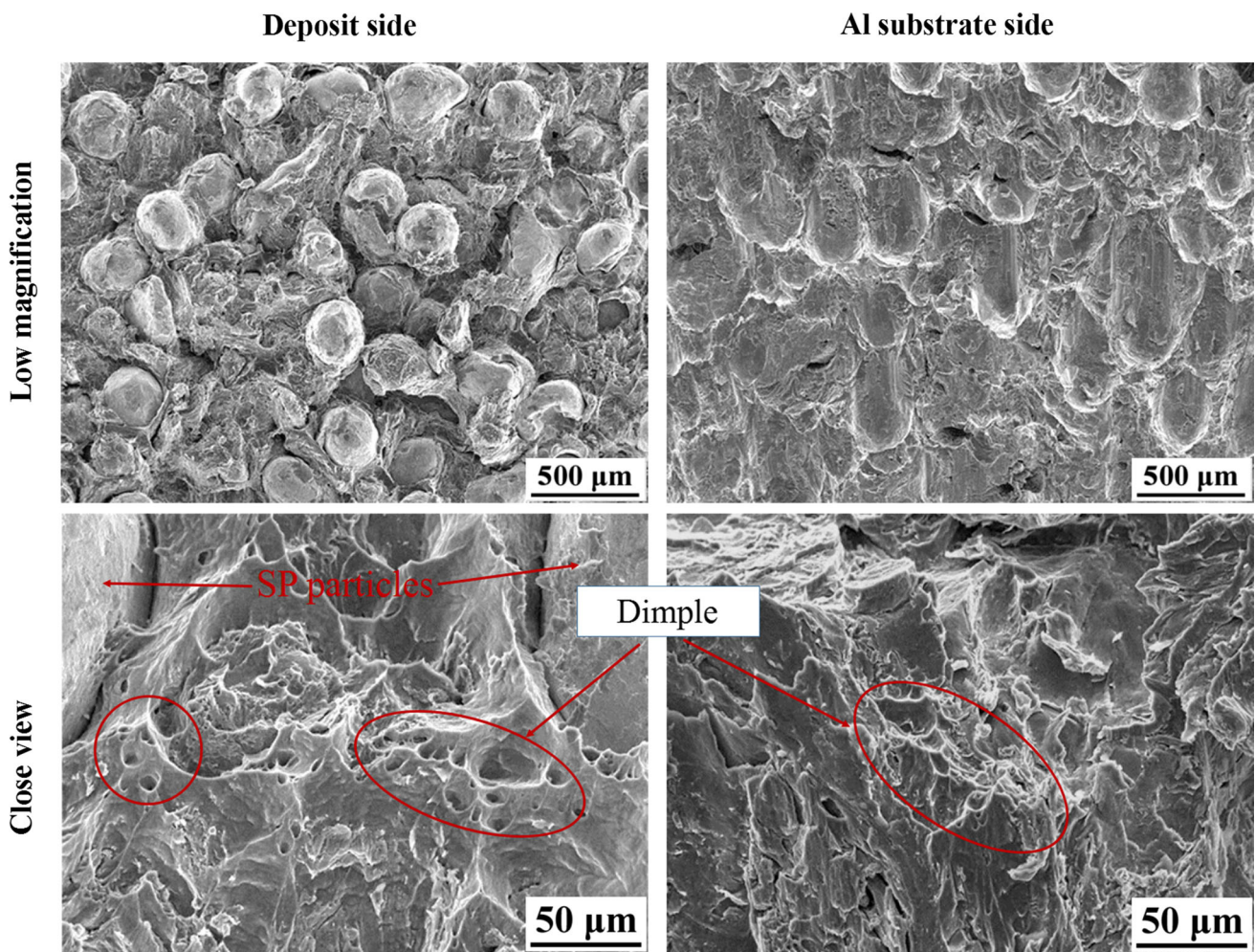


Fig. 26 Morphologies of the tensile fractures of substrate/deposit interfaces sprayed with powder mixtures containing 70 vol.% shot peen particles

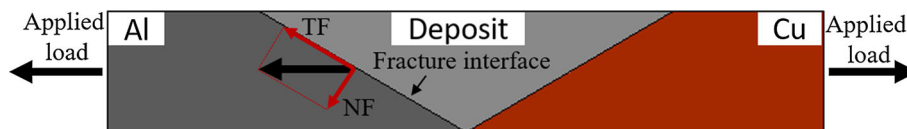


Fig. 27 Schematic of the force analysis in the tensile test. *TF* tangential force, *NF* normal force

- 12.4 to 0.2%, and the microhardness was significantly improved.
- The shear strength of deposit/Cu and deposit/Al interfaces increased gradually with an increase in shot peen particle content. The minimum shear strength was 8.8 ± 1.1 MPa (Cu) and 8.4 ± 1.8 MPa (Al) for the Al layer deposited without shot peen particles, and the maximum shear strength was 90 ± 5.6 MPa (Cu) and 68 ± 5.8 MPa (Al), for the layer deposited with powder mixtures containing 70 vol.% shot peen particles. When pure Al was deposited using powder mixtures that contained 10 and 30 vol.% shot peen

- particles, the shear strength of the deposit/Al interface was greater than that of the deposit/Cu interface. When the shot peen particle content was increased to 50 and 70 vol.%, the shear strength of the deposit/Al interface was less than that of the deposit/Cu interface.
- When the spray angle decreased from 90° to 45° , the deposition efficiency of a mixture containing pure Al powder + 70 vol.% shot peen particles significantly decreased, and the shear strength of the deposit/Cu and deposit/Al interfaces decreased from 90 ± 5.6 to 78 ± 3.5 MPa for the deposit/Cu interface and from 68 ± 5.8 to 55 ± 3.1 MPa for the deposit/Al interface.

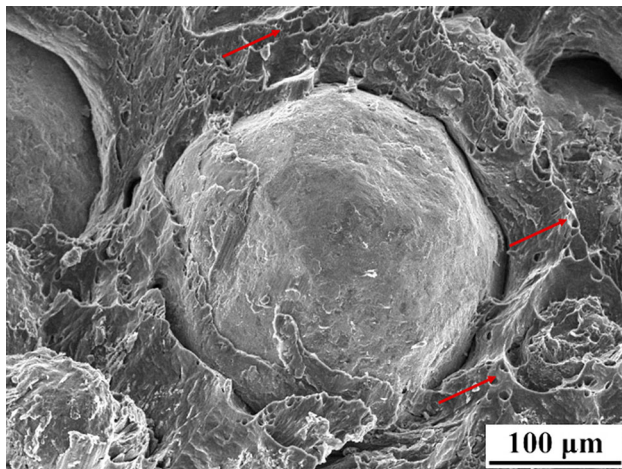


Fig. 28 Morphology of the tensile fractures of a deposited Al particle near a shot peen particle

4. The average tensile strength of the Al-Cu joint prepared using CSB is about 71.4 ± 1.5 MPa, and the initial fracture location is at the deposit/Al interface. Dimples on the tensile failure indicate that ductile rupture occurred during the fracture process. In situ shot peen-assisted cold spraying is a novel method that opens a new way for joining dissimilar materials.

Acknowledgment This research was supported by the National Natural Science Foundation of China (No. 51761145108).

References

- S.D. Meshram, T. Mohandas, and G.M. Reddy, Friction Welding of Dissimilar Pure Metals, *J. Mater. Process. Technol.*, 2007, **184**(1-3), p 330-337
- K.P. Mehta and V.J. Badheka, A Review on Dissimilar Friction Stir Welding of Copper to Aluminum: Process, Properties, and Variants, *Mater. Manuf. Process.*, 2015, **31**(3), p 233-254
- Z. Sun and R. Karppi, The Application of Electron Beam Welding for the Joining of Dissimilar Metals: An Overview, *J. Mater. Process. Technol.*, 1996, **59**(3), p 257-267
- J.E. Lee, D.H. Bae, W.S. Chung, K.H. Kim, J.H. Lee, and Y.R. Cho, Effects of Annealing on the Mechanical and Interface Properties of Stainless Steel/Aluminum/Copper Clad-Metal Sheets, *J. Mater. Process. Technol.*, 2007, **187-188**, p 546-549
- J.-P. Immariageon, R.T. Holt, A.K. Koul, L. Zhao, W. Wallace, and J.C. Beddoes, Lightweight Materials for Aircraft Applications, *Trans. Indian Inst. Met.*, 2016, **70**(1), p 125-131
- A. Safarzadeh, M. Paidar, and H. Youzbashi-zade, A Study on the Effects Bonding Temperature and Holding Time on Mechanical and Metallurgical Properties of Al-Cu Dissimilar Joining by DFW, *Trans. Indian Inst. Met.*, 2016, **70**(1), p 125-131
- M. Akbari, P. Bahemmat, M. Haghpanahi, and M.K. Besharati, Givi, Enhancing Metallurgical and Mechanical Properties of Friction Stir Lap Welding of Al-Cu Using Intermediate Layer, *Sci. Technol. Weld. Join.*, 2013, **18**(6), p 518-524
- H.J. Liu, J.J. Shen, S. Xie, Y.X. Huang, F. Cui, C. Liu, and L.Y. Kuang, Weld Appearance and Microstructural Characteristics of Friction Stir Butt Barrier Welded Joints of Aluminium Alloy to Copper, *Sci. Technol. Weld. Join.*, 2013, **17**(2), p 104-110
- H.J. Liu, J.J. Shen, L. Zhou, Y.Q. Zhao, C. Liu, and L.Y. Kuang, Microstructural Characterisation and Mechanical Properties of Friction Stir Welded Joints of Aluminium Alloy to Copper, *Sci. Technol. Weld. Join.*, 2013, **16**(1), p 92-98
- I. Galvão, J.C. Oliveira, A. Loureiro, and D.M. Rodrigues, Formation and Distribution of Brittle Structures in Friction Stir Welding of Aluminium and Copper: Influence of Shoulder Geometry, *Intermetallics*, 2012, **22**, p 122-128
- J. Nishiwaki, T. Kambe, Y. Kedo, Y. Harada, S. Muraishi, and S. Kumai, Numerical Analysis of Wavy Interface Formation and Successive Temperature Change in Magnetic Pulse Welded Al/Cu Joint, *Mater. Sci. Forum*, 2016, **877**, p 655-661
- W. Shi, W. Wang, and Y. Huang, Laser Micro-welding of Cu-Al Dissimilar Metals, *Int. J. Adv. Manuf. Technol.*, 2015, **85**(1-4), p 185-189
- P.C. Seshagiri, G. Madhusudan Reddy, K. Srinivasa Rao, M. Govinda Raju, S.S. Bhattacharya, and K. Prasad Rao, Microstructure and Mechanical Properties of Sc modified Al-Cu Alloy (AA2219) Electron Beam Welds, *Sci. Technol. Weld. Join.*, 2013, **13**(5), p 415-421
- B. Gulenc, Investigation of Interface Properties and Weldability of Aluminum and Copper Plates by Explosive Welding Method, *Mater. Des.*, 2008, **29**(1), p 275-278
- M. Sedighi and M. Honarpisheh, Experimental Study of Through-Depth Residual Stress in Explosive Welded Al-Cu-Al Multilayer, *Mater. Des.*, 2012, **37**, p 577-581
- H. Amani and M. Soltanieh, Intermetallic Phase Formation in Explosively Welded Al/Cu Bimetals, *Metal. Mater. Trans. B*, 2016, **47**(4), p 2524-2534
- C.Z. Xia, Y.J. Li, J. Wang, and H.J. Ma, Microstructure and Phase Constitution Near Interface of Cu/Al Vacuum Brazing, *Mater. Sci. Technol.*, 2013, **23**(7), p 815-818
- J. Peng, S. Fukumoto, L. Brown, and N. Zhou, Image Analysis of Electrode Degradation in Resistance Spot Welding of Aluminium, *Sci. Technol. Weld. Join.*, 2013, **9**(4), p 331-336
- M.N. Avettand-Fenoël, R. Taillard, G. Ji, and D. Goran, Multiscale Study of Interfacial Intermetallic Compounds in a Dissimilar Al 6082-T6/Cu Friction-Stir Weld, *Metal. Mater. Trans. A*, 2012, **43**(12), p 4655-4666
- I. Galvão, A. Loureiro, D. Verdera, D. Gesto, and D.M. Rodrigues, Influence of Tool Offsetting on the Structure and Morphology of Dissimilar Aluminum to Copper Friction-Stir Welds, *Metal. Mater. Trans. A*, 2012, **43**(13), p 5096-5105
- P. Xue, B.L. Xiao, D.R. Ni, and Z.Y. Ma, Enhanced Mechanical Properties of Friction Stir Welded Dissimilar Al-Cu Joint by Intermetallic Compounds, *Mater. Sci. Eng. A*, 2010, **527**(21-22), p 5723-5727
- C.W. Tan, Z.G. Jiang, L.Q. Li, Y.B. Chen, and X.Y. Chen, Microstructural Evolution and Mechanical Properties of Dissimilar Al-Cu Joints Produced by Friction Stir Welding, *Mater. Des.*, 2013, **51**, p 466-473
- P. Xue, D.R. Ni, D. Wang, B.L. Xiao, and Z.Y. Ma, Effect of Friction Stir Welding Parameters on the Microstructure and Mechanical Properties of the Dissimilar Al-Cu Joints, *Mater. Sci. Eng. A*, 2011, **528**(13-14), p 4683-4689
- R.C. Dykhuizen and M.F. Smith, Gas Dynamic Principles of Cold Spray, *J. Therm. Spray Technol.*, 1998, **7**(2), p 205-212
- M. Grujicic, C.L. Zhao, C. Tong, W.S. DeRosset, and D. Helfrich, Analysis of the Impact Velocity of Powder Particles in the Cold-Gas Dynamic-Spray Process, *Mater. Sci. Eng. A*, 2004, **368**(1-2), p 222-230

26. H. Assadi, F. Gärtner, T. Stoltenhoff, and H. Kreye, Bonding Mechanism in Cold Gas Spraying, *Acta Mater.*, 2003, **51**(15), p 4379-4394
27. R. Ghelichi, D. MacDonald, S. Bagherifard, H. Jahed, M. Guagliano, and B. Jodoin, Microstructure and Fatigue Behavior of Cold Spray Coated Al5052, *Acta Mater.*, 2012, **60**(19), p 6555-6561
28. W.Y. Li, D.D. Zhang, C.J. Huang, S. Yin, M. Yu, F.F. Wang, and H.L. Liao, Modelling of Impact Behaviour of Cold Spray Particles: Review, *Surf. Eng.*, 2014, **30**(5), p 299-308
29. X. Meng, J. Zhang, J. Zhao, Y. Liang, and Y. Zhang, Influence of Gas Temperature on Microstructure and Properties of Cold Spray 304SS Coating, *J. Mater. Sci. Technol.*, 2011, **27**(9), p 809-815
30. V.K. Champagne, M.K. West, M. Reza Rokni, T. Curtis, V. Champagne, and B. McNally, Joining of Cast ZE41A Mg to Wrought 6061 Al by the Cold Spray Process and Friction Stir Welding, *J. Therm. Spray Technol.*, 2015, **25**(1-2), p 143-159
31. X.-T. Luo, C.-X. Li, F.-L. Shang, G.-J. Yang, Y.-Y. Wang, and C.-J. Li, High Velocity Impact Induced Microstructure Evolution During Deposition of Cold Spray Coatings: A Review, *Surf. Coat. Technol.*, 2014, **254**, p 11-20
32. H. Bu, M. Yandouzi, C. Lu, D. MacDonald, and B. Jodoin, Cold Spray Blended Al+Mg17Al12 Coating for Corrosion Protection of AZ91D Magnesium alloy, *Surf. Coat. Technol.*, 2012, **207**, p 155-162
33. E. Sansoucy, P. Marcoux, L. Ajdelsztajn, and B. Jodoin, Properties of SiC-Reinforced Aluminum Alloy Coatings Produced by the Cold Gas Dynamic Spraying Process, *Surf. Coat. Technol.*, 2008, **202**(16), p 3988-3996
34. Y.-K. Wei, X.-T. Luo, C.-X. Li, and C.-J. Li, Optimization of in situ Shot-Peening-Assisted Cold Spraying Parameters for Full Corrosion Protection of Mg Alloy by Fully Dense Al-Based Alloy Coating, *J. Therm. Spray Technol.*, 2016, **26**(1-2), p 173-183
35. X.-T. Luo, Y.-K. Wei, Y. Wang, and C.-J. Li, Microstructure and Mechanical Property of Ti and Ti6Al4 V Prepared by an in situ Shot Peening Assisted Cold Spraying, *Mater. Des.*, 2015, **85**, p 527-533
36. Z. Arabgol, H. Assadi, T. Schmidt, F. Gärtner, and T. Klassen, Analysis of Thermal History and Residual Stress in Cold-Sprayed Coatings, *J. Therm. Spray Technol.*, 2013, **23**(1-2), p 84-90
37. S. Cho, K. Takagi, H. Kwon, D. Seo, K. Ogawa, K. Kikuchi, and A. Kawasaki, Multi-walled Carbon Nanotube-reinforced Copper Nanocomposite Coating Fabricated by Low-pressure Cold Spray Process, *Surf. Coat. Technol.*, 2012, **206**(16), p 3488-3494
38. S. Dosta, M. Couto, and J.M. Guilemany, Cold Spray Deposition of a WC-25Co Cermet onto Al7075-T6 and Carbon Steel Substrates, *Acta Mater.*, 2013, **61**(2), p 643-652
39. H. Lee and K. Ko, Effect of SiC Particle Size on Cold Sprayed Al-SiC Composite Coatings, *Surf. Eng.*, 2013, **25**(8), p 606-611
40. K. Spencer, D.M. Fabijanic, and M.X. Zhang, The Use of Al-Al₂O₃ Cold Spray Coatings to Improve the Surface Properties of Magnesium Alloys, *Surf. Coat. Technol.*, 2009, **204**(3), p 336-344
41. C.-J. Li and W.-Y. Li, Deposition Characteristics of Titanium Coating in Cold Spraying, *Surf. Coat. Technol.*, 2003, **167**(2-3), p 278-283
42. B.S. Deforce, T.J. Eden, and J.K. Potter, Cold Spray Al-5% Mg Coatings for the Corrosion Protection of Magnesium Alloys, *J. Therm. Spray Technol.*, 2011, **20**(6), p 1352-1358
43. M. Diab, X. Pang, and H. Jahed, The Effect of Pure Aluminum Cold Spray Coating on Corrosion and Corrosion Fatigue of Magnesium (3% Al-1% Zn) Extrusion, *Surf. Coat. Technol.*, 2016, **309**, p 423-435
44. E. Irissou, J.G. Legoux, B. Arsenaault, and C. Moreau, Investigation of Al-Al₂O₃ Cold Spray Coating Formation and Properties, *J. Therm. Spray Technol.*, 2007, **16**(5-6), p 661-668
45. G. Li, X.-F. Wang, and W.-Y. Li, Effect of Different Incidence Angles on Bonding Performance in Cold Spraying, *Trans. Nonferr. Met. Soc. Chin.*, 2007, **17**(1), p 116-121
46. C.-J. Li, W.-Y. Li, Y.-Y. Wang, G.-J. Yang, and H. Fukanuma, A Theoretical Model for Prediction of Deposition Efficiency in Cold Spraying, *Thin Solid Films*, 2005, **489**(1-2), p 79-85
47. C. Otten, U. Reisgen, and M. Schmachtenberg, Electron Beam Welding of Aluminum to Copper: Mechanical Properties and Their Relation to Microstructure, *Weld. World*, 2015, **60**(1), p 21-31
48. Q.-Z. Zhang, W.-B. Gong, and W. Liu, Microstructure and Mechanical Properties of Dissimilar Al-Cu Joints by Friction Stir Welding, *Trans. Nonferr. Met. Soc. Chin.*, 2015, **25**(6), p 1779-1786
49. S.A. Khodir, M.M.Z. Ahmed, E. Ahmed, S.M.R. Mohamed, and H. Abdel-Aleem, Effect of Intermetallic Compound Phases on the Mechanical Properties of the Dissimilar Al/Cu Friction Stir Welded Joints, *J. Mater. Eng. Perform.*, 2016, **25**(11), p 4637-4648
50. P. Xue, B. Xiao and Z. Ma, Microstructure and Mechanical Properties of Friction Stir Welded Dissimilar Al-Cu Thin Plate Joints, in *10th International Symposium on Friction Stir Welding* (Beijing, 2014)
51. A. Esmaeili, M.K.B. Givi, and H.R.Z. Rajani, Investigation of Weld Defects in Dissimilar Friction stir Welding of Aluminium to Brass by Radiography, *Sci. Technol. Weld. Join.*, 2013, **17**(7), p 539-543
52. A. Esmaeili, H.R. Zareie Rajani, M. Sharbati, M.K.B. Givi, and M. Shamanian, The Role of Rotation Speed on Intermetallic Compounds Formation and Mechanical Behavior of Friction Stir Welded Brass/Aluminum 1050 Couple, *Intermetallics*, 2011, **19**(11), p 1711-1719
53. A. Esmaeili, M.K.B. Givi, and H.R.Z. Rajani, A Metallurgical and Mechanical Study on Dissimilar Friction Stir welding of Aluminum 1050 to Brass (CuZn30), *Mater. Sci. Eng. A*, 2011, **528**(22-23), p 7093-7102
54. L. Qiao, H.H. Yang, and J.F. Sheng, Comparison Study on Friction-Welded Cu-Al Material and Pure Cu/Al, *Mater. Sci. Forum*, 2015, **817**, p 374-378
55. M.F.X. Muthu and V. Jayabalan, Tool Travel Speed Effects on the Microstructure of Friction Stir Welded Aluminum-Copper Joints, *J. Mater. Process. Technol.*, 2015, **217**, p 105-113
56. D. Yaduwanshi, S. Pal, and S. Bag, Effect of Preheating on Mechanical Properties of Hybrid Friction Stir Welded Dissimilar Joint, in *5th International and 26th All India Manufacturing Technology, Design and Research Conference (AIMTDR)* (Assam, 2014)
57. R. Sarrafi, A.H. Kokabi, M.A. Gharacheh, and B. Shalchi, Evaluation of Microstructure and Mechanical Properties of Aluminum to Copper Friction Stir Butt Welds, *Frict. Stir Weld. Process.*, 2011, **VI**, p 253-264
58. M. Girard, B. Huneau, C. Genevois, X. Sauvage, and G. Racineux, Friction Stir Diffusion Bonding of Dissimilar Metals, *Sci. Technol. Weld. Join.*, 2013, **15**(8), p 661-665
59. W.-B. Lee, K.-S. Bang, and S.-B. Jung, Effects of Intermetallic Compound on the Electrical and Mechanical Properties of Friction Welded Cu/Al Bimetallic Joints During Annealing, *J. Alloys Compd.*, 2005, **390**(1-2), p 212-219
60. P. Eslami and A.K. Taheri, An Investigation on Diffusion Bonding of Aluminum to Copper Using Equal Channel Angular Extrusion Process, *Mater. Lett.*, 2011, **65**(12), p 1862-1864
61. Z. Huiwen, C. Wei, H. Jingshan, Y. Jiuchun, and Y. Shiqin, Formation and Evolution of Intermetallic Compounds at Interfaces of Cu/Al Joints by Ultrasonic-Assisted Soldering, *J. Mater. Process. Technol.*, 2015, **223**, p 1-7

62. Y. Xiao, H. Ji, M. Li, and J. Kim, Ultrasound-Assisted Brazing of Cu/Al Dissimilar Metals Using a Zn-3Al Filler Metal, *Mater. Des.*, 2013, **52**, p 740-747
63. Z. Ni, H. Zhao, P. Mi, and F. Ye, Microstructure and Mechanical Performances of Ultrasonic Spot Welded Al/Cu Joints with Al 2219 Alloy Particle Interlayer, *Mater. Des.*, 2016, **92**, p 779-786
64. J. Feng, X. Songbai, and D. Wei, Reliability Studies of Cu/Al Joints Brazed with Zn-Al-Ce Filler Metals, *Mater. Des.*, 2012, **42**, p 156-163
65. T. Solchenbach, P. Plapper, and W. Cai, Electrical Performance of Laser Braze-Welded Aluminum-Copper Interconnects, *J. Manuf. Process.*, 2014, **16**(2), p 183-189
66. T. Solchenbach and P. Plapper, Mechanical Characteristics of Laser Braze-welded Aluminium-Copper Connections, *Opt. Laser Technol.*, 2013, **54**, p 249-256
67. I. Bhamji, R.J. Moat, M. Preuss, P.L. Threadgill, A.C. Addison, and M.J. Peel, Linear Friction Welding of Aluminium to Copper, *Sci. Technol. Weld. Join.*, 2013, **17**(4), p 314-320